ASM Sc. J., 12, Special Issue 4, 2019 for ICSE2018, 90-96

Separation of Red Blood Cells along the Planar Plane using Castellated and Straight Electrodes

Farahdiana Wan Yunus, Muhammad Ramdzan Buyong, Jumril Yunas, Burhanudin Yeop Majlis and Azrul Azlan Hamzah*

Institute of Microengineering and Nanoelectronics (IMEN),

Universiti Kebangsaan Malaysia,

43600 Bangi, Selangor, Malaysia

In this research work, the dielectrophoresis (DEP) technique was applied on the membrane of an artificial kidney. Two electrodes, i.e., castellated and straight electrodes, were designed and used to separate red blood cells (RBC) from membranes with the DEP technique. The primary objective of this paper was to clear the centre of the membranes. The results from the simulations and experiments were compared to determine if the simulations were acceptable. Additionally, the distribution and the intensity of the electric field were also compared between the castellated and straight electrodes. Higher electric field intensity and better electric field distributions from the results were compared to select the best electrode for use in an artificial kidney. The result for the castellated electrode's electric field was $4.23e^5$ V/m, while that of the straight electrode was $2.27e^5$ V/m. The electric field distribution for the castellated electrode was $4.81e^5$ V/m, while that for the straight electrode was $2.36e^5$ V/m. Both the electric field intensity and the electric field distributions showed that the castellated electrodes achieved much better results. Additionally, the movement of the RBC also showed movement along the electric field lines. In summary, the castellated electrodes were deemed to be the best option for use in an artificial kidney, as the simulation results showed.

Keywords: dielectrophoresis, castellated electrodes, straight electrodes, DEP, red blood cells, RBC, electric fields

I. INTRODUCTION

Dielectrophoresis (DEP) refers to the movement of particles in a non-uniform electric field due to time variation (AC) (Buyong *et al.*, 2015). Dielectrophoresis can be controlled by the frequency, electrical properties, and the size and shape of the particles. When an electric field, *E,* is applied, the dielectric particles behave as an effective dipole with the dipole moment, ρ, directly proportional to the electric field (Buyong *et al.*, 2014),

$$\rho \, \alpha \, E \tag{1}$$

In general, the proportional constant depends on the shape and size of the dielectric particles. The force of the dipole moment is shown in equation 2 below, when an electric field gradient is applied (Buyong *et al.*, 2017; Yunus *et al.*, 2018),

$$F = (\rho.d)\, E = k\, E \tag{2}$$

where, ρ is the dipole moment vector of the constant, d is the del vector, k is the induced dipole moment, and E is the external electric field. In order to derive the constant k, the dielectrophoresis force (F_{DEP}) equation is shown below (equation 3) (Buyong *et al.*, 2014; Yunus *et al.*, 2017),

$$F_{DEP} = 2\pi\varepsilon_{medium}\, R^3\, CMF\, (dE^2) \tag{3}$$

*Corresponding author's e-mail: azlanhamzah@ukm.edu.my

where, ε_m is the permittivity of the medium, dE is the gradient, rms, of the electric field, and r is the radius of the particle. The most crucial part for DEP relates to the Clausius-Mossotti factor (CMF) as given by (Buyong *et al.*, 2014),

$$CMF = (\varepsilon_{particle} - \varepsilon_{medium}) / (\varepsilon_{particle} - 2\varepsilon_{medium}) \quad (4)$$

ε_{medium} and $\varepsilon_{particle}$ are the complex permittivity particles in the medium and cells (Buyong *et al.*, 2015). The CMF can be calculated using MATLAB software.

DEP has been widely used in the medical industry for various applications such as clinical cell sorting (Martinez-Duarte, 2012) biological cell separation (Pohl, 1977; De Gasperis *et al.*, 1999), and the manipulation of biological cells (Gagnon, 2011). Numerous biological cells have been successfully separated, manipulated and sorted using DEP techniques, such as cancer cells (Sonnenberg *et al.*, 2014), DNA (Song *et al.*, 2015), human leukocytes (Yang *et al.*, 2000), CD34+ cell subpopulation from bone marrow (Talary *et al.*, 1995), and peripheral blood stem cells (Talary *et al.*, 1995). It has been proven that red blood cells can be implemented in an artificial kidney to separate biological waste. Research by (Buyong *et al.*, 2016) described the possibility of implementing DEP in the glomerular filtration of an artificial kidney. In short, this paper showcases simulation results using the COMSOL Multiphysics 5.2 electric field against experimental trials to prove that the results were acceptable for medical use. Two electrodes designs, i.e., castellated and straight, are described in this paper. Blood droplets will be used to test the movement in the electric field.

II. ELECTRODE DESIGNS

An AC/DC electric field module from the COMSOL Multiphysics version 5.2 was used to simulate the electric field across both electrode designs. Figure 1 below shows an image of the electrodes with the straight design (a.) and castellated design (b.).

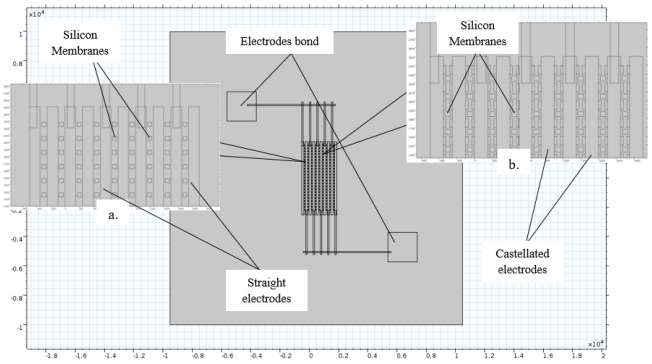

Figure 1. Design of the electrodes using simulation software; a. straight electrodes b. castellated electrodes

Subsequently, the electric fields for both the electrodes were compared using software and experimental data.

III. FABRICATION DESIGNS

In this paper, two lithography steps were used. First, lithography was used for the fabrication of the membranes, and secondly, for the fabrication of the electrodes. Figure 2a and Figure 2b below shows the images of the fabricated castellated (Abidin *et al.*, 2013) and straight electrodes. The castellated electrodes were designed to have finger tips in between the membranes, while the straight electrodes did not have these finger tips in them.

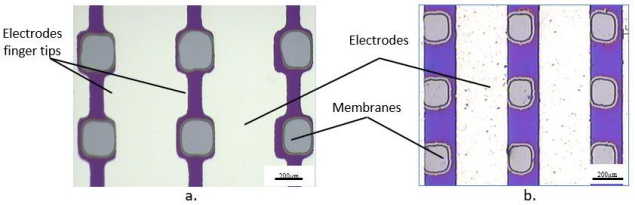

Figure 2. a. Fabricated castellated electrodes design b. fabricated straight electrodes design

The first part of the fabrication took place using standard cleaning to ensure that the samples were free of any impurities. Subsequently, the lithography step was employed. Each sample was coated with a photoresist to form a pattern of the membranes, as shown in Figure 3b, Then, silicon nitride on the membranes was fully etched using a buffer oxide etching solution (BOE) (Yunas, Hamzah and Majlis, 2009), as shown in Figure 3c. In the second part of the lithography process, the samples were deposited with aluminium to form the electrodes (Hamzah,

Majlis and Ahmad, 2004; Hamzah *et al.*, 2008) (Figure 3d.), which was later removed (Figure 3e.) using acetone. Figure 3 below shows the schematic figure of the fabrication process.

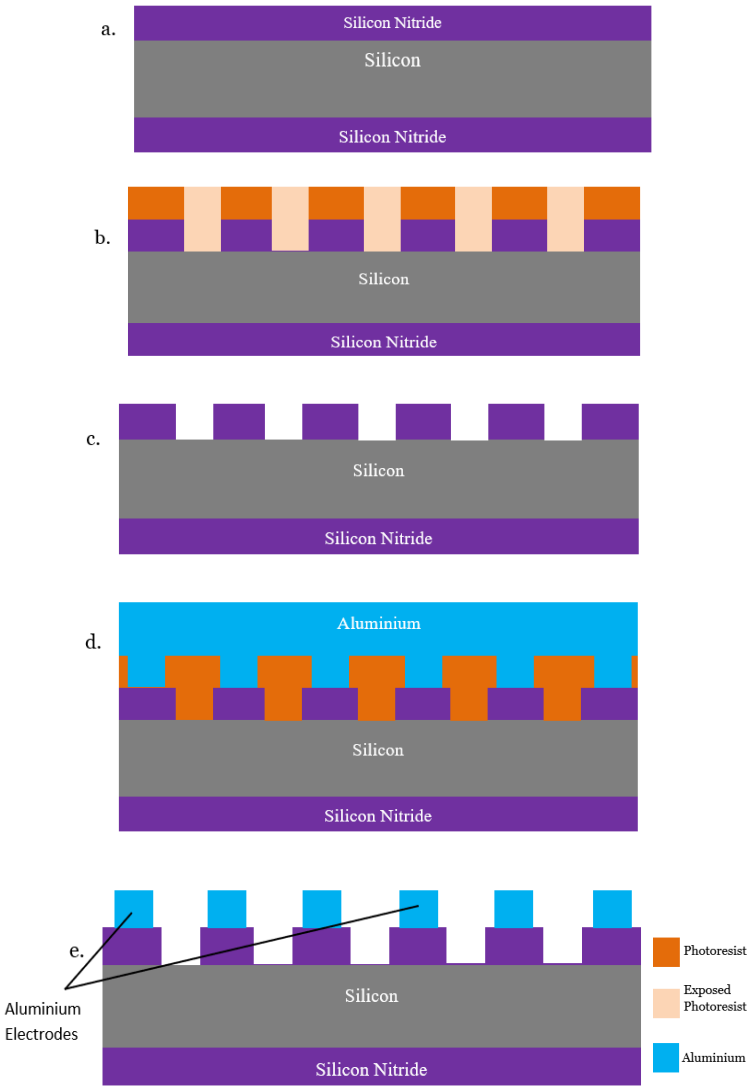

Figure 3. a. silicon wafer coated with silicon nitride on the top and bottom, b. exposure of the resist on the membranes, c. silicon nitride etching using BOE, d. photoresist coating and aluminium sputtered on top of the sample and the photoresist, e. removal process to form the electrodes

The illustration of the experimental setup is shown in Figure 4. The probes were directly connected to the electrodes and the function generator. A voltage of 10V was applied and the opposing side was grounded. As the experiment used biological particles, RBC, the electric potential should not be higher than 10V to avoid the particles from being damaged. Therefore, 10V was chosen because it had the clearest image of the particle's movement. The electrodes were then observed under a microscope with a droplet of red blood cell (RBC) on top of it. The blood droplet's movement was observed to compare it with that of the electric field lines in the simulation results.

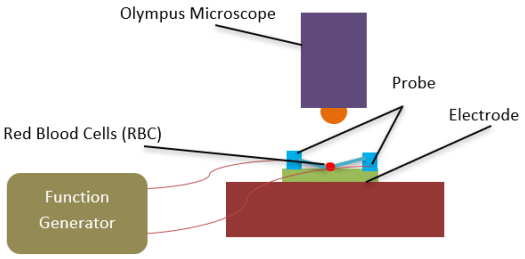

Figure 4. Illustration of experimental setup

IV. RESULTS AND DISCUSSION

A. Comsol Multiphysics

Simulation (Marsi *et al.*, 2014) results showed that the electric fields of the castellated electrodes were much higher compared to that of the straight electrodes. The highest surface electric field for the straight electrode was recorded at $2.27e^5$ V/m, while that of the castellated electrodes was recorded at $4.23e^5$ V/m. Figure 5a. and 5b. show the electric field lines for the castellated and straight electrodes.

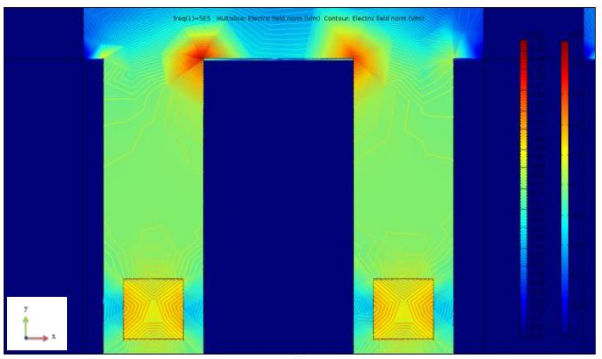

a.

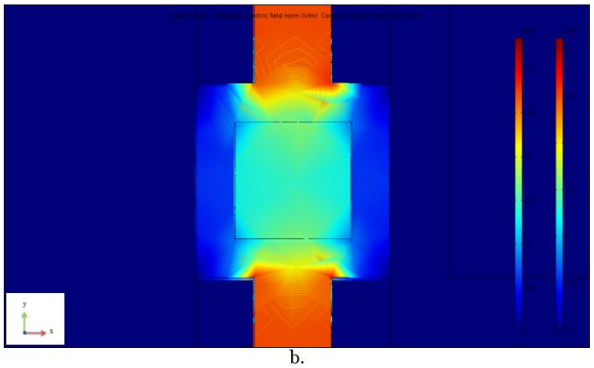

b.

Figure 5. a. electric field lines for the straight electrodes, b. electric field lines for the castellated electrodes

The electric field lines for the straight electrodes show that the electric fields were highest at the centre of the silicon membranes, while for the castellated electrodes, the highest intensity of the electric fields was at the edge of the castellated electrodes. As for the electric field distribution, the results of the simulations are shown in Figure 6a and Figure 6b. The highest volume of the electric field for the castellated electrodes was at $4.81e^5$ V/m, while that for the straight electrodes was at $2.36e^5$ V/m.

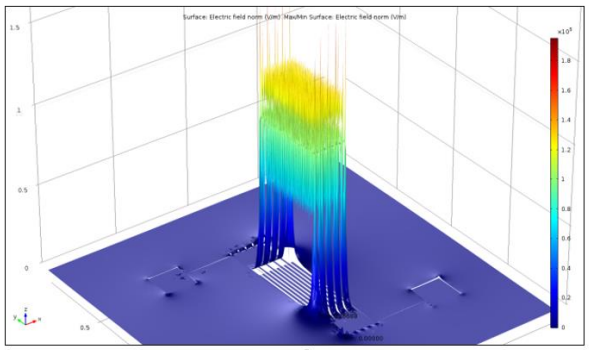

a.

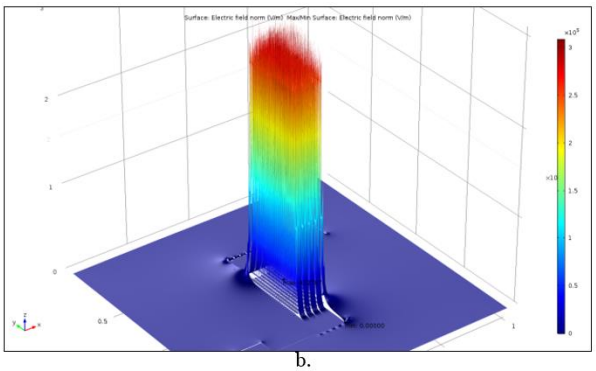

b.

Figure 6. a. electric field distributions of the straight electrodes, b. electric field distributions of the castellated electrodes

The electric field distributions show that the castellated electrodes had a much higher electric field as indicated by the deeper orange shade, as compared to the distributions across the straight electrodes. The results in Figures 5 and 6 showed that the castellated electrodes had a much higher electric field. Notably, the distance between the castellated electrodes were much closer, the electric field was much stronger, and the electric field distribution was uniform. These results indicated a much better performance. Equation 5 below shows the relationship between the electric field, E, and the distance between the electrodes, d:

$$E = kQ/d^2 \quad (5)$$

The electric fields are inversely proportional to the distance between the electrodes; d. Closer electrodes produce much higher electric fields. Furthermore, sharp edges tend to have much higher electric fields due to the smaller surface area. The smaller the surface area, the higher the accumulation of electrons in the area, thus generating a much greater charge. This brings about a much greater magnitude and higher electric field in this area.

B. Experimental

Figure 7 below shows images of the particle's movements responding to the electric field; Figure 5a for the straight electrodes, and Figure 5b for the castellated electrodes.

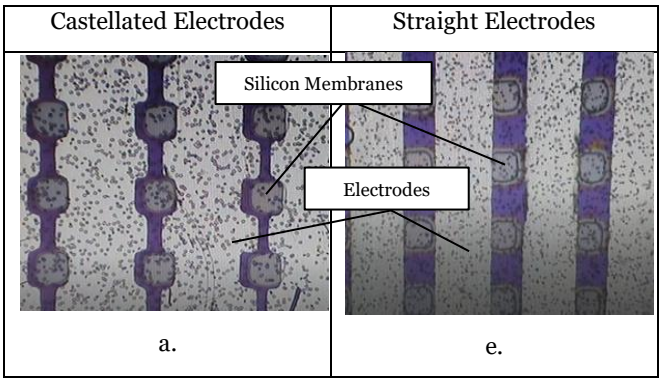

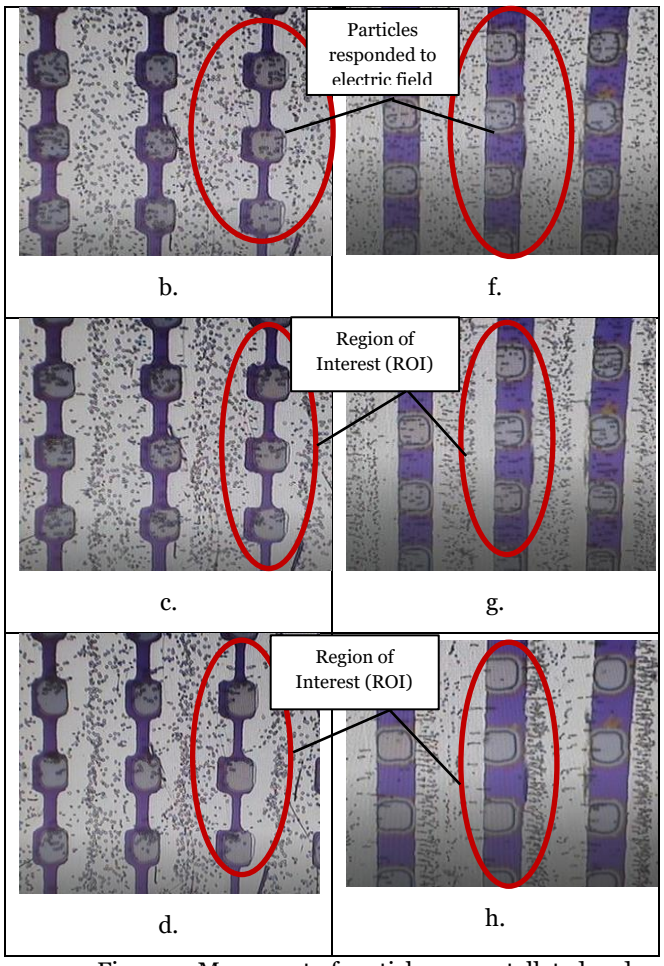

Figure 7. Movement of particles on castellated and straight electrodes

The particles for both the electrodes in Figures 7a and 7e were uniform in nature, before the electric field was applied. The RBC started to respond as shown in Figures 7b and 7f after the function generator was switched on. The region of interest (ROI) was the region required for this study. Having said that, the silicon membrane parts were identified as the required ROI. The particles in Figure 7c moved towards the high electric field, which was the edge of the castellated electrodes (see Figure 5b). The particles cleared the membranes by moving towards the edge as per Figure 7d. As for the straight electrodes, the high electric field was at the centre of the membrane (see Figure 5a). Thus, as soon as the electric field was applied, the particles responded and moved toward the centre, as shown in Figure 7g, before starting to separate and clear the membranes(Figure 7h).

Therefore, the results of electric field obtained from simulations were proven to fit that of the particles in the experiment. The particles moved across the electric field when it was triggered. The results from the volume and surface electric fields indicated that the castellated electrodes had a much higher electric field because the overall results from the timing of the particle's movement indicated that the castellated electrodes were much more efficient and led to a faster response from the particles.

V. CONCLUSIONS

The castellated electrodes had a much higher electric field at $4.23e^5$ V/m, a superior electric field distribution ($4.81e^5$ V/m), and separated the particles the fastest. As for the movement of the particles, it is proven that the simulation results were acceptable because the particles responded to the electric fields. The particles have been successfully shown to be able to be separated from the membranes. Thus, this application can be implemented in artificial kidneys.

VI. ACKNOWLEDGEMENT

The authors would like to acknowledge the sponsorship from the Fabrication of Silicon Membrane Filtration System for Artificial Kidney which was funded through the SKIM GERAN PENYELIDIKAN PEMBANGUNAN PROTOTAIP (PRGS), the HICOE-AKU-95 grant which was funded by The Ministry of Higher Education, and the DPP-2018-006 Peranti Bioperubatan with IOT which was funded through the Dana Pembangunan Penyelidikan PTJ, as well as the PRGS/1/2017/TK05/UKM/02/1 Design grant.

VII. REFERENCES

Abidin, HEZ *et al.* 2013, 'Electrical characteristics of double stacked ppy-pva supercapacitor for powering biomedical mems devices', *Microelectronic Engineering*. Elsevier B.V., 111, pp. 374–378. doi: 10.1016/j.mee.2013.03.057.

Buyong, MR *et al.* 2014, 'Finite element modeling of dielectrophoretic microelectrodes based on a array and ratchet type', 2014 *IEEE International Conference on Semiconductor Electronics, Proceedings, ICSE*, pp. 236–239. doi: 10.1109/SMELEC.2014.6920840.

Buyong, MR *et al.* 2015, 'A tapered aluminium microelectrode array for improvement of dielectrophoresis-based particle manipulation', *Sensors*, vol. 15, no. 5, pp. 10973–10990. doi: 10.3390/s150510973.

Buyong, MR *et al.* 2016, 'Implementing the concept of dielectrophoresis in glomerular filtration of human kidneys', *Proceedings of IEEE International Conference on Semiconductor Electronics,* pp. 33–37. doi: 10.1109/SMELEC.2016.7573584.

Buyong, MR *et al.* 2017, 'Determination of lateral and vertical dielectrophoresis forces using tapered microelectrode array', *Micro & Nano Letters*, vol. 2, pp. 1–6. doi: 10.1049/mnl.2017.0542.

Gagnon, ZR 2011, 'Cellular dielectrophoresis: Applications to the characterization, manipulation, separation and patterning of cells', *Electrophoresis*, vol. 32, no. 18, pp. 2466–2487. doi: 10.1002/elps.201100060.

De Gasperis, G *et al.* 1999, 'Microfluidic cell separation by 2-dimensional dielectrophoresis', *Biomedical Microdevices*, vol. 2, no. 1, pp. 41–49. doi: 10.1023/A:1009955200029.

Hamzah, AA *et al.* 2008, 'Sputtered encapsulation as wafer level packaging for isolatable MEMS devices: A technique demonstrated on a capacitive accelerometer', *Sensors*, vol. 8, no. 11, pp. 7438–7452. doi: 10.3390/s8117438.

Hamzah, AA , Majlis, BY & Ahmad, I 2004, 'Deflection analysis of epitaxially deposited polysilicon encapsulation for MEMS devices', *Proceedings of* 2004 *International Conference in Semiconductor Electronics*, pp. 611–614.

Marsi, N *et al.* 2014, 'The mechanical and electrical effects of MEMS capacitive pressure sensor based 3C-SiC for extreme temperature', *Journal of Engineering (United States)*, 2014. doi: 10.1155/2014/715167.

Martinez-Duarte, R 2012, 'Microfabrication technologies in dielectrophoresis applications-A review', *Electrophoresis*, vol. 33, no. 21, pp. 3110–3132. doi: 10.1002/elps.201200242.

Pohl, HA 1977, 'Dielectrophoresis : applications to the characterization and separation of cells', in *Methods of Cell Separation*, pp. 67-169, (d). doi: 10.1007/978-1-4684-0820-1_3.

Song, Y *et al.* 2015, 'Device for dielectrophoretic separation and collection of nanoparticles and DNA under high conductance conditions', *Electrophoresis*, vol. 36, no. 9, pp. 1107–1114. doi: 10.1002/elps.201400507.

Sonnenberg, A *et al.* 2014, 'rapid electrokinetic isolation of cancer-related circulating cell-free DNA directly from blood, *Clinical Chemistry*, vol. 60, no. 3, doi: 10.1373/clinchem.2013.214874.

Talary, MS *et al.* 1995, 'Dielectrophoretic separation and enrichment of CD34+cell subpopulation from bone marrow and peripheral blood stem cells', *Medical & Biological Engineering & Computing*, vol. 33, no. 2, pp. Pp. 235–237. doi: 10.1007/BF02523050.

Yang, J *et al.* 2000, 'Differential analysis of human leukocytes by dielectrophoretic field- flow-fractionation', *Biophysical Journal*, vol. 78, no. 5, pp. 2680–2689. doi: 10.1016/S0006-

3495(00)76812-3.

Yunas, J, Hamzah, AA & Majlis, BY 2009, 'Surface micromachined on-chip transformer fabricated on glass substrate', *Microsystem Technologies*, vol. 15, no. 4, pp. 547–552. doi: 10.1007/s00542-008-0704-2.

Yunus, FW *et al.* 2017, 'Negative charge dielectrophoresis by using different radius of electrodes for biological particles', *Proceedings of the 2017 IEEE Regional Symposium on Micro and Nanoelectronics,* pp. 84–87. doi: 10.1109/RSM.2017.8069126.

Yunus, FW *et al.* 2018, 'Dielectrophoresis : iron dificient anemic red blood cells for artificial kidney purposes', *2018 IEEE International Conference on Semiconductor Electronics (ICSE)*, pp. 5–8. doi: 10.1109/SMELEC.2018.8481205.